

Fine-scale tribological performance of zeolitic imidazolate framework (ZIF-8) based polymer nanocomposite membranes

Nay Win Khun,¹ E. M. Mahdi,² Siqi Ying,² Tan Sui,²
 Alexander M. Korsunsky,² and Jin-Chong Tan^{2,a}

¹*School of Mechanical and Aerospace Engineering, Nanyang Technological University, 50 Nanyang Avenue, Singapore 639798, Singapore*

²*Department of Engineering Science, University of Oxford, Parks Road, Oxford OX1 3PJ, United Kingdom*

(Received 29 July 2014; accepted 23 August 2014; published online 13 October 2014)

We combined zeolitic imidazolate framework nanoparticles (ZIF-8: ~150 nm diameter) with Matrimid® 5218 polymer to form permeable mixed matrix membranes, featuring different weight fractions of nanoparticles (up to 30 wt. % loading). We used ball-on-disc micro-tribological method to measure the frictional coefficient of the nanocomposite membranes, as a function of nanoparticle loading and annealing heat treatment. The tribological results reveal that the friction and wear of the unannealed samples rise steadily with greater nanoparticle loading because ZIF-8 is relatively harder than the matrix, thus promoting abrasive wear mechanism. After annealing, however, we discover that the nanocomposites display an appreciably lower friction and wear damage compared with the unannealed counterparts. Evidence shows that the major improvement in tribological performance is associated with the greater amounts of wear debris derived from the annealed nanocomposite membranes. We propose that detached Matrimid-encapsulated ZIF-8 nanoparticles could function as “spacers,” which are capable of not only reducing direct contact between two rubbing surfaces but also enhancing free-rolling under the action of lateral forces. © 2014 Author(s). All article content, except where otherwise noted, is licensed under a Creative Commons Attribution 3.0 Unported License. [<http://dx.doi.org/10.1063/1.4897280>]

Metal-organic frameworks (MOFs) are nanoporous crystalline materials constructed from inorganic and organic building blocks via molecular self-assembly yielding a myriad of 3-D open framework structures.¹ MOFs offer a wide range of physico-chemical properties, especially noted for their high surface area combined with chemical tunability² and framework flexibility.³ Fabrication of MOF-based membranes and thin-film coatings has provided novel platforms for emergent technologies encompassing gas separation, water purification, sensors, and low-*k* dielectrics.^{4–7}

Polyimides are ideal for membrane applications by virtue of their high gas permeability and intrinsic permselectivity (e.g., CO₂/N₂, H₂/CO₂, and H₂/CH₄) compared to polycarbonate, polysulfone, and other polymeric materials. The gas transport performance of polyimide membranes can be further enhanced by cross-linking modification,⁸ which also stabilizes the material against thermal and chemical degradation. Matrimid® 5218 is an example of a high-performance polyimide, featuring attractive combination of gas permeability and selectivity,⁹ in combination with high glass transition temperature and excellent mechanical properties.¹⁰

Interestingly, recent studies have demonstrated that the incorporation of MOFs, particularly zeolitic imidazolate frameworks (ZIFs) into certain polymers, such as Matrimid^{11–13} and Polydimethylsiloxane (PDMS),¹⁴ could improve the resulting composites permeability and selectivity critical to

^ajin-chong.tan@eng.ox.ac.uk

membrane applications. For example, Song *et al.*¹¹ recently reported that ZIF nanoparticles could enhance diffusion of gasses through their porous cages in addition to the creation of free volume by disrupting the molecular packing of Matrimid, both of which yield an improvement in permeability. This novel grade of MOF-based nanocomposite membranes belongs to a rapidly growing research area, termed “mixed matrix membranes” (MMMs).^{15,16} It is surprising that relatively little is known about the mechanical behaviour of MOF-based MMMs,^{13,17} particularly concerning their tribological behavior. Indeed, good tribological performance is key to enable many industrial-scale applications, not only during the membrane manufacturing and packaging steps but also to warrant durability and extended lifetime in service.¹⁸ Hitherto, there are only two reports associated with the wear behaviour of MOF-type materials. Shi *et al.*¹⁹ investigated the tribological behavior of ZIF-8 and ZIF-67 as additives in liquid lubricants, both of which appear to demonstrate promising anti-wear property. More recently, Van de Voorde *et al.*²⁰ evaluated the effects of interfacial adhesion strength of polycrystalline MOF thin-film coatings, in the context of their scratch and wear resistance behavior via the nanoscratch method. While knowledge of tribological performance of MOF-based membranes is important to ascertain their robustness for commercial deployment, this is an area that is yet to be explored. This work, therefore, represents the first study of its kind to elucidate the fine-scale tribological characteristics of a prototypical MOF-based MMM material.

In this work, ZIF-8 nanoparticles were incorporated into Matrimid 5218 at different loadings (in wt. %) to form ZIF-8@Matrimid MMM.¹¹ The ZIF-8 nanoparticles (mean diameter ~150 nm) were synthesized using the rapid room temperature synthesis method, as described in Cravillon *et al.*,²¹ 0.3 g of $\text{Zn}(\text{NO}_3)_2 \cdot 6\text{H}_2\text{O}$ (procured from Fischer Scientific and used as is) was mixed with 0.66 g of 2-methylimidazole (Fischer Scientific) in 10 ml methanol each and stirred for an hour at room temperature, where a milky white precipitate was observed to form after a few minutes. The precipitate was separated from the solution via centrifugation (8000 rpm for 10 min), dispersed and kept suspended in chloroform for the preparation of the MMM. Matrimid 5218 (Huntsman) was dissolved in chloroform and stirred for 24–48 h to ensure its complete dissolution. Hereafter, the previously synthesized ZIF-8 nanoparticles were mixed with the dissolved Matrimid in measured amounts to form solutions with different weight percentage loadings of ZIF-8 nanoparticles (0 to 30 wt. %). These mixtures were left to stir for another 24–48 h in order to ensure complete and uniform dispersion of the nanoparticles into Matrimid. The resulting nanocomposite solutions were then cast with the doctor-blade method at a speed of 10 mm s^{-1} to form membranes with an average thickness of *ca.* 100–150 μm . These membranes were dried overnight in a glove bag saturated with chloroform vapour, after which they were transferred to a vacuum oven and dried at 60°C for 24 h. After drying, samples were annealed at 150°C under vacuum for another 24 h. We note that the variation in membrane thickness upon annealing is typically small at ~1%.

The cross-sectional morphology of the resulting ZIF-8@Matrimid nanocomposite membranes was characterized using scanning electron microscopy (FEG-SEM, Tescan LYRA3 in the Oxford Multi-Beam Laboratory for Engineering Microscopy (MBLEM)) at a magnification of 50–100 k \times (10–15 keV). Cross-sections of the membranes were prepared by breaking the samples immersed in a liquid nitrogen bath. Fig. 1 shows the typical microstructures at the cross-sections of the

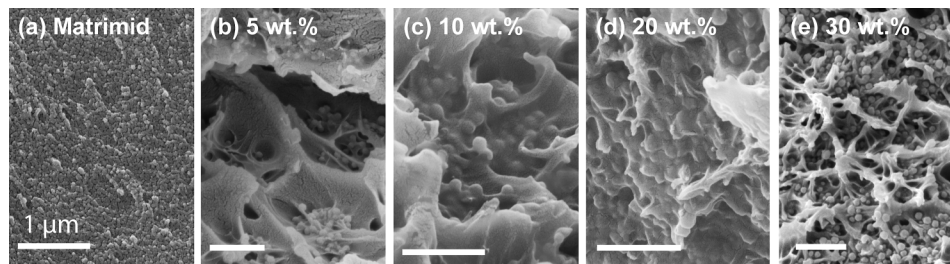


FIG. 1. SEM micrographs showing typical cross-sectional morphology of unannealed ZIF-8@Matrimid membranes. (a) Matrimid. (b)–(e) Nanocomposites with nanoparticle loading of 5, 10, 20, and 30 wt. %, respectively. The scale bar represents 1 μm .

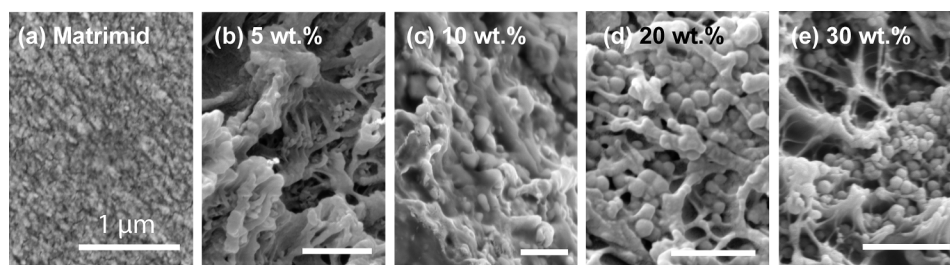


FIG. 2. SEM micrographs showing typical cross-sectional morphology of annealed ZIF-8@Matrimid membranes. (a) Matrimid. (b)-(e) Nanocomposites with different ZIF-8 loadings of 5, 10, 20, and 30 wt. %, respectively. The scale bar denotes 1 μm .

unannealed MMMs. cursory inspection across all of the samples revealed that the incorporation of ZIF-8 nanoparticles into Matrimid (the polymer matrix) seems to have proceeded rather well, where the majority of nanoparticles have been individually “encapsulated” (coated)²² with Matrimid. The dispersion of ZIF-8 nanoparticles into Matrimid also seems to be uniform across all membranes. There are, however, certain regions in the membranes that reveal segregation of ZIF-8 nanoparticles not well incorporated into the Matrimid matrix, which may have been caused by the nanoparticles “settling” during the stirring or drying process. This is especially pronounced at higher loadings exceeding ~ 20 wt. % of nanoparticles, where more nanoparticle aggregates have been identified (Fig. 1(e)). We note that the introduction of ZIF-8 nanoparticles seems to interrupt the microstructural coherency and packing¹¹ of the Matrimid matrix, as exemplified in Fig. 1(e), thereby giving rise to microscopic voids within the otherwise continuous membrane structure.

While similar trends have been observed for the annealed nanocomposite membranes (Fig. 2), a distinct feature is that the microscopic voids that are present in the unannealed samples are less pronounced after subjecting the membranes to a subsequent annealing heat treatment step. Annealing of samples in vacuum may have improved the interfacial bonding between Matrimid and ZIF-8 nanoparticles, while ridding the membrane of entrapped solvents and gases. The annealed samples appear to be more homogeneous, suggesting that macromolecular rearrangements have taken place to stabilize the initially disarrayed microstructure. Similar to its unannealed counterpart, higher loadings of ZIF-8 yielded more unblended nanoparticles (see Fig. 2(e)) that become exposed and thus segregated from the polymeric matrix.

The fine-scale tribological behaviour of the ZIF-8@Matrimid nanocomposites was investigated using the ball-on-disc micro-tribometer (CSM Instruments, ASTM G99 and G133 standards). Unlubricated sliding wear tests were performed on the membrane surfaces against a Cr6 steel ball (diameter 6 mm) for up to ~ 3000 laps, in a circular path of 2 mm in diameter, at a sliding speed of 1 cm s^{-1} and under a normal load of 1 N. All tests were conducted at room temperature (RT $\sim 23^\circ\text{C}$). Prior to micro-tribological testing, the nanocomposite membranes ($1 \times 1 \text{ cm}^2$) were carefully bonded onto laboratory glass slides using an epoxy glue and left to cure at RT for four days. Fig. 3 presents the evolution of the frictional coefficients (μ) for unannealed and annealed ZIF-8@Matrimid MMMs, plotted as a function of the number of sliding wear laps. We note that, at higher ZIF-8 nanoparticle loading (wt. %), both categories of membranes exhibit relatively higher frictional coefficients throughout the entire duration of testing. Notably, we established that the annealed membranes show consistently lower frictional coefficient than their unannealed counterparts.

Fig. 4 shows the averaged frictional coefficients (μ) of the unannealed and annealed MMMs as a function of ZIF-8 loading. For the unannealed membranes, it can be seen that there is a marked increase in μ from ~ 0.36 to 0.51 , by raising the nanoparticles loading from 0 to 30 wt. %. This ascending trend can be understood by comparing the indentation hardness property of ZIF-8 ($H \sim 530 \text{ MPa}$)²³ against that of the softer (unannealed) Matrimid ($H \sim 260 \text{ MPa}$),²⁴ from which it is evident that ZIF-8 nanoparticles are approximately twice as hard as the unannealed matrix material. On this basis, we anticipate that abrasive wear behavior will be enhanced by integrating a higher content of ZIF-8 as part of the nanocomposite. To this end, membranes containing higher nanoparticle content (i.e., more asperities) produce higher friction since a larger contact area is established

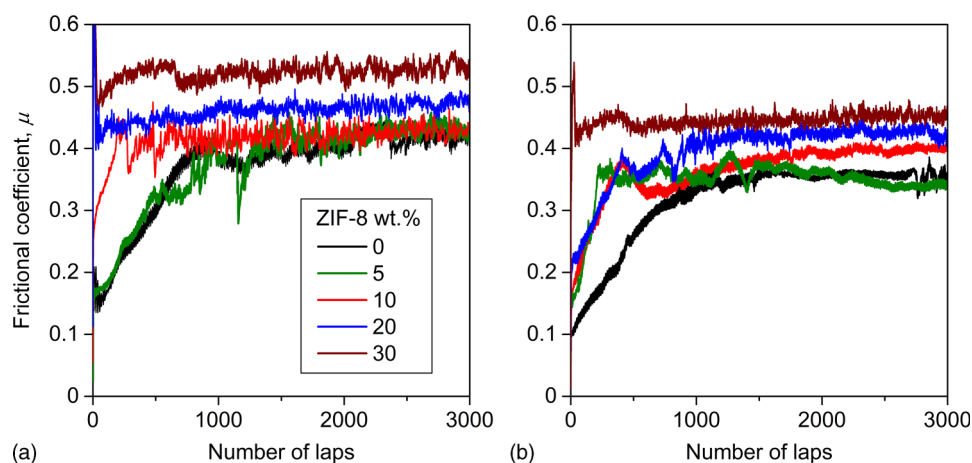


FIG. 3. Frictional coefficients of ZIF-8@Matrimid nanocomposites as a function of the number of laps in the ball-on-disc sliding wear tests, for (a) unannealed and (b) annealed membranes. The circular path of each lap has a diameter of 2 mm.

between the two rubbing surfaces; this result is in line with previous studies (e.g., Refs. 25–28). In a similar fashion, the tribological data indicate that raising the loading of ZIF-8 from 0 to 30 wt. % increases the frictional coefficient of annealed membranes from ~ 0.32 to 0.46 (Fig. 4). It is striking to see that the annealed nanocomposites exhibit lower frictional coefficients across all compositions versus their unannealed counterparts. This phenomenon can be explained by noting an increase in the hardness of the annealed Matrimid ($H \sim 330$ MPa),²⁴ which translates into an approximately 30% rise in the overall hardness of Matrimid due to microstructural densification upon annealing. Conversely, we note that the framework structure of ZIF-8 remains stable up to *ca.* 450 °C, such that its hardness value is not affected by the annealing step at 150 °C.^{23,29}

By means of surface contact profilometry (Talyscan-150, equipped with a diamond stylus of 4 μm diameter), we have characterized the basic dimensions of the wear tracks as a function of nanoparticle loading and annealing condition. Fig. 5 shows that by increasing ZIF-8 loading, the width and depth of the wear track dimensions detected on unannealed samples have both doubled, confirming that the wear rate of (softer) membranes is exacerbated by raising the content of (harder) ZIF-8. Such an outcome is expected given the swift increase in frictional coefficient

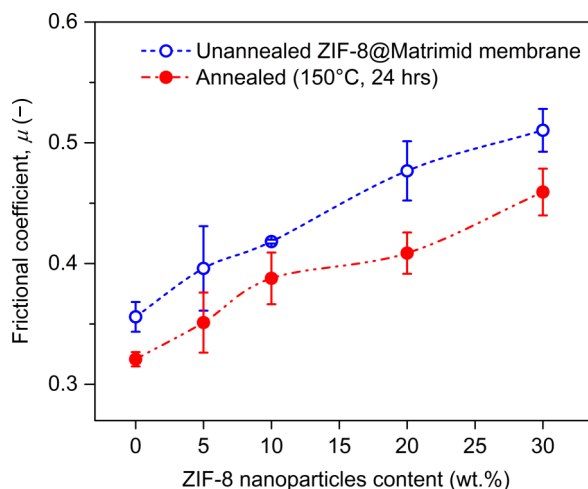


FIG. 4. Frictional coefficients of ZIF-8@Matrimid nanocomposites as a function of nanoparticle content, for unannealed and annealed membranes. Three measurements per sample were carried out to determine the average value of μ . The dotted lines are guides for the eye, highlighting the upward trend.

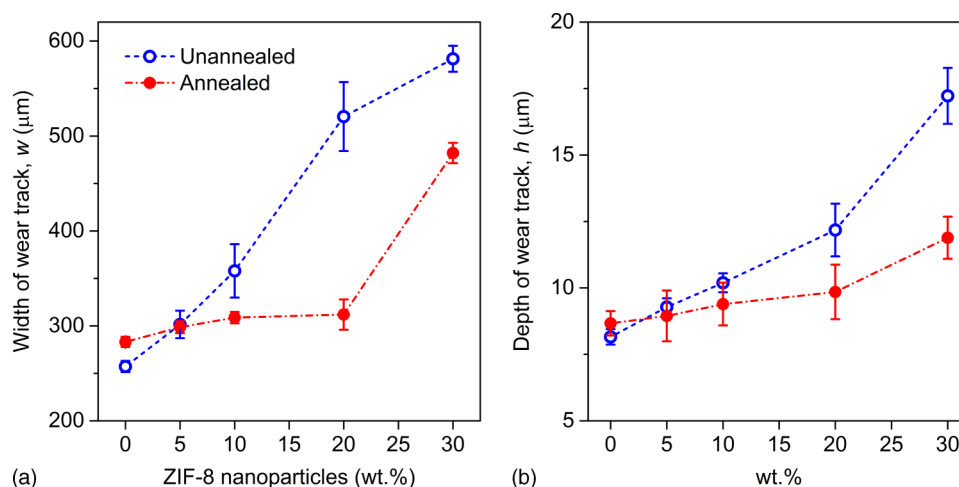


FIG. 5. Changes in wear track geometry in terms of the (a) width and (b) depth, both as a function of ZIF-8 nanoparticle content and heat treatment condition.

with nanoparticle loading (Fig. 4). Surprisingly, we discover that the trend is completely different for the annealed membranes, whose corresponding values are substantially lower (Fig. 5). This unexpected result highlights the major improvement in abrasive wear performance at ZIF-8 loading exceeding ~ 5 wt.%. Particularly up to ~ 20 wt.%, it is impressive to see that the wear behavior of the annealed nanocomposites (harder matrix) is largely unaffected by the nanoparticle content, despite a persistent increase witnessed in their accompanying frictional coefficients (Fig. 4). Wear increases drastically from 20 to 30 wt.%, which might be linked to the extensive segregation of uncoated ZIF-8 nanoparticles (Fig. 2(e)).

To gain insights into the wear mechanisms, we have examined the surface morphology of the worn ZIF-8@Matrimid membranes using scanning electron microscopy (JEOL-JSM-5800), in conjunction with surface contact profilometry to extract detailed 3-D surface topography. The

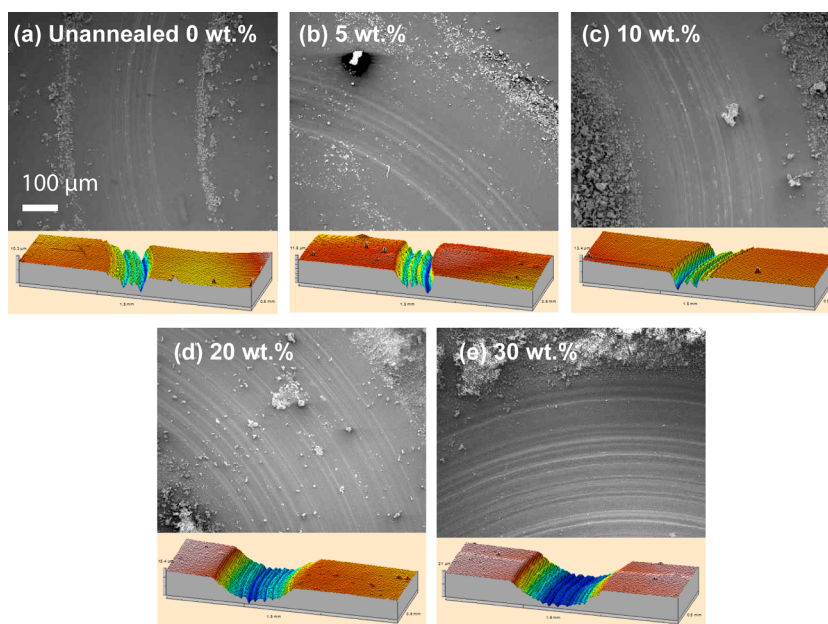


FIG. 6. SEM micrographs accompanied by 3-D surface profiles of unannealed membranes after ball-on-disc tests at 3000 laps (diameter 2 mm, sliding speed 1 cm s^{-1} , and normal load 1 N). The accompanying 3-D profilometry images do not exhibit buildup of wear debris since the stylus operating under contact mode has displaced loose particles lying on its path.

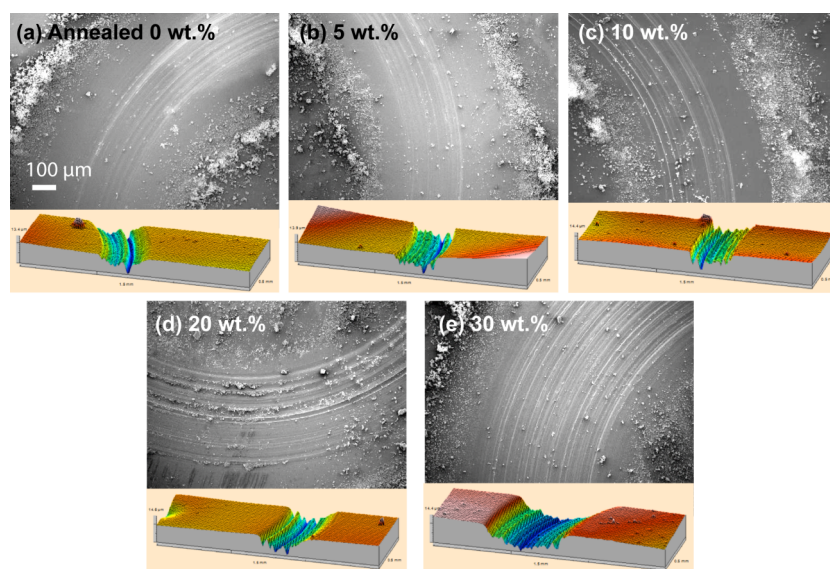


FIG. 7. SEM micrographs and 3-D surface profiles of annealed membranes after being subjected to 3000 laps using the ball-on-disc micro-tribometer. Note the substantially larger amounts of wear debris being generated on the wear tracks compared with those in Fig. 6 (with same parameters).

results of the unannealed samples are presented in Fig. 6, where significantly larger wear tracks can be directly linked to the increasing ZIF-8 loading. It is noted that the abrasive scars found on the wear tracks are produced by repeated sliding of the Cr6 steel ball, which points to the predominant abrasive wear mechanism. On the contrary, it can be seen that the annealed membranes generate a noticeably larger amount of wear debris on their wear tracks (Fig. 7). In light of this finding, we postulate that annealing of Matrimid yields microstructural changes that could facilitate the removal of ZIF-8 nanoparticles from the annealed matrix (which exhibits greater hardness but lower ductility),²⁴ through the mechanism of abrasive wear in sliding mode. However, the ZIF-8 nanoparticles coated with Matrimid that are being “released” (detached) from the matrix form fine-scale wear debris, which bridge the gap between two rubbing interfaces to aid in further reduction of friction (Fig. 4). Our results suggest that such debris function as “spacers” capable of suppressing damage caused by abrasive wear, by promoting free rolling and sliding contact mechanisms^{27,28} under action of lateral forces.

In summary, we have systematically investigated, for the first time, the micro-tribological behavior of a prototypical mixed matrix membrane comprising ZIF-8@Matrimid nanocomposites. It was found that the *annealed* membranes exhibit markedly lower friction and wear behavior compared with their unannealed counterparts. We further demonstrate that an optimal wear resistance performance of the annealed membranes can be obtained at 5–20 wt. % nanoparticle loading. In essence, we discover that fine debris of ZIF-8 nanoparticles encapsulated with Matrimid could facilitate the sliding-rolling contact mechanism, thus offering enhanced protection against unlubricated abrasive wear. This result bodes well for gas-adsorption and separation oriented applications because the *annealed* ZIF-8@Matrimid membranes not only show outstanding gas permeation properties,¹¹ but also excellent wear resistance performance. It will be rewarding for future work to explore the wear performance of mixed matrix membranes which incorporate MOFs featuring a range of porosity levels, architectures and chemical structures, and to investigate the effects of temperature on wear performance.

E.M.M. would like to thank Yayasan Khazanah for funding his D.Phil. studies that made this work possible in the Department of Engineering Science at the University of Oxford. A.M.K. acknowledges funding received for the MBLEM Laboratory at Oxford through the EU FP7 Project iSTRESS (604646). J.C.T. and E.M.M. are grateful to Mr. V.T. Dickinson at Huntsman Advanced Materials (Europe) for provision of the Matrimid samples.

- ¹ N. Stock and S. Biswas, *Chem. Rev.* **112**(2), 933–969 (2012).
- ² D. N. Bunck and W. R. Dichtel, *Chem. - Eur. J.* **19**(3), 818–827 (2013).
- ³ A. Ghoufi, A. Subercaze, Q. Ma, P. G. Yot, Y. Ke, I. Puente-Orench, T. Devic, V. Guillermin, C. Zhong, C. Serre, G. Férey, and G. Maurin, *J. Phys. Chem. C* **116**(24), 13289–13295 (2012).
- ⁴ J.-R. Li, J. Sculley, and H.-C. Zhou, *Chem. Rev.* **112**(2), 869–932 (2012).
- ⁵ J.-Y. Lee, C. Y. Tang, and F. Huo, *Sci. Rep.* **4**, 3740 (2014).
- ⁶ L. E. Kreno, K. Leong, O. K. Farha, M. Allendorf, R. P. Van Duyne, and J. T. Hupp, *Chem. Rev.* **112**(2), 1105–1125 (2012).
- ⁷ M. R. Ryder and J.-C. Tan, *Mater. Sci. Tech.* **30**(13a), 1598–1612 (2014).
- ⁸ L. Shao, T.-S. Chung, S. H. Goh, and K. P. Pramoda, *J. Membr. Sci.* **238**(1–2), 153–163 (2004).
- ⁹ A. C. Comer, D. S. Kalika, B. W. Rowe, B. D. Freeman, and D. R. Paul, *Polymer* **50**(3), 891–897 (2009).
- ¹⁰ N. Carmen, S. Sergey, P. Marcel, and P. N. Suzana, *Environ. Eng. Manage. J.* **7**(6), 653–659 (2008).
- ¹¹ Q. Song, S. K. Nataraj, M. V. Roussanova, J. C. Tan, D. J. Hughes, W. Li, P. Bourgoignie, M. A. Alam, A. K. Cheetham, S. A. Al-Muhtaseb, and E. Sivaniah, *Energy Environ. Sci.* **5**(8), 8359–8369 (2012).
- ¹² S. Japip, H. Wang, Y. Xiao, and T. Shung Chung, *J. Membr. Sci.* **467**, 162–174 (2014).
- ¹³ M. J. C. Ordoñez, K. J. Balkus, Jr., J. P. Ferraris, and I. H. Musselman, *J. Membr. Sci.* **361**(1–2), 28–37 (2010).
- ¹⁴ H. Fan, Q. Shi, H. Yan, S. Ji, J. Dong, and G. Zhang, *Angew. Chem. Int. Ed. Engl.* **53**(22), 5578–5582 (2014).
- ¹⁵ G. X. Dong, H. Y. Li, and V. K. Chen, *J. Mater. Chem. A* **1**(15), 4610–4630 (2013).
- ¹⁶ I. Erucar, G. Yilmaz, and S. Keskin, *Chem.-Asian J.* **8**(8), 1692–1704 (2013).
- ¹⁷ S. Liu, R. Ananthoji, S. Han, B. Knudsen, X. Li, L. Wojtas, J. Massing, C. V. Gauthier, and J. P. Harmon, *New J. Chem.* **36**(7), 1449 (2012).
- ¹⁸ J. C. Tan and A. K. Cheetham, *Chem. Soc. Rev.* **40**(2), 1059–1080 (2011).
- ¹⁹ Q. Shi, Z. F. Chen, Z. W. Song, J. P. Li, and J. X. Dong, *Angew. Chem. Int. Ed.* **50**(3), 672–675 (2011).
- ²⁰ B. Van de Voorde, R. Ameloot, I. Stassen, M. Everaert, D. De Vos, and J. C. Tan, *J. Mater. Chem. B* **1**(46), 7716–7724 (2013).
- ²¹ J. Cravillon, S. Munzer, S.-J. Lohmeier, A. Feldhoff, K. Huber, and M. Wiebcke, *Chem. Mater.* **21**(8), 1410–1412 (2009).
- ²² See supplementary material at <http://dx.doi.org/10.1063/1.4897280> for additional SEM micrographs and 3-D surface profiles.
- ²³ J. C. Tan, T. D. Bennett, and A. K. Cheetham, *Proc. Natl. Acad. Sci. U. S. A.* **107**(22), 9938–9943 (2010).
- ²⁴ E. M. Mahdi and J. C. Tan, Manuscript in preparation, in which indentation hardness of Matrimid has been measured using the nanoindentation method outlined in Ref. 23.
- ²⁵ F. Svahn, A. Kassman-Rudolphi, and E. Wallen, *Wear* **254**(11), 1092–1098 (2003).
- ²⁶ P. L. Menezes, Kishore, and S. V. Kailas, *Wear* **267**(9–10), 1534–1549 (2009).
- ²⁷ T. S. Barrett, G. W. Stachowiak, and A. W. Batchelor, *Wear* **153**(2), 331–350 (1992).
- ²⁸ N. W. Khun and E. Liu, *Tribol. Trans.* **55**(4), 401–408 (2012).
- ²⁹ J.-C. Tan, B. Civalleri, C.-C. Lin, L. Valenzano, R. Galvelis, P.-F. Chen, T. D. Bennett, C. Mellot-Draznieks, C. M. Zicovich-Wilson, and A. K. Cheetham, *Phys. Rev. Lett.* **108**(9), 095502 (2012).